Influence of Isotherm Inflection on the Loading Dependence of the Diffusivities of *n*-Hexane and *n*-Heptane in MFI Zeolite. Quasi-Elastic Neutron Scattering Experiments Supplemented by Molecular Simulations

H. Jobic,[†] N. Laloué,[†,‡] C. Laroche,[‡] J. M. van Baten,[§] and R. Krishna*[,§]

Institut de Recherches sur la Catalyse, CNRS, 2 avenue A. Einstein, 69626 Villeurbanne, France, Institut Français du Pétrole, BP 3, 69390 Vernaison, France, and Van 't Hoff Institute for Molecular Sciences, University of Amsterdam, Nieuwe Achtergracht 166, 1018 WV Amsterdam, The Netherlands

Received: October 5, 2005; In Final Form: November 25, 2005

Quasi-Elastic Neutron Scattering (QENS) experiments were carried out to determine (a) Fick diffusivity, D (b) self-diffusivity, D_{self}, and (c) $1/\Gamma$, the inverse of the thermodynamic correction factor, for *n*-hexane (nC6) and *n*-heptane (nC7) in MFI zeolite (all silica silicalite-1) at 300 K for a variety of loadings. These experimental results are compared with configurational-bias Monte Carlo (CBMC) and molecular dynamics (MD) simulations of, respectively, the adsorption isotherms and diffusivities. For *n*-hexane, the CBMC simulated isotherm shows a slight inflection at a loading $\Theta = 4$ molecules per unit cell; this inflection manifests, also, in the loading dependence of $1/\Gamma$, obtained from QENS. The trend in the loading dependence of the Fick D and D_{self} of nC6 obtained from QENS matches the MD simulation results. For nC7 the CBMC simulated isotherm shows a strong inflection at a loading $\Theta = 4$ molecules per unit cell. At this loading $\Theta = 4$, $1/\Gamma$ tends to zero and there is a very good match between QENS and molecular simulations for the loading dependence of $1/\Gamma$. Both MD simulations and QENS data on the Fick diffusivity shows a sharp maximum at a loading in the region of $\Theta = 4$. For both nC6 and nC7 the simulated values of diffusivity are about an order of magnitude higher than those determined from QENS.

1. Introduction

Zeolites are widely used as catalysts and adsorbents in a variety of applications in the chemical and petrochemical industries.[1] For the design of catalytic and separation processes employing zeolites it is necessary to have accurate information on the transport, or Fick, diffusivity D of guest molecules, defined for one-component diffusion by[2]

$$\mathbf{N} = -\rho D \nabla \Theta \tag{1}$$

In eq 1, $\mathbf{N}$ is the molecular flux, Θ is molecular loading expressed in, for example, molecules per unit cell, and ρ is the zeolite framework density expressed as the number of unit cells per m^3. In the alternative Maxwell−Stefan (M−S) approach[2−4] the chemical potential gradient $\nabla\mu$ is used as the driving force and the M−S diffusivity $Đ$ is defined by

$$\mathbf{N} = -\rho\Theta Đ \frac{1}{RT}\nabla\mu \tag{2}$$

In eq 2, R is the gas constant and T is the temperature. The Fick and M−S diffusivities are inter-related

$$D = Đ\Gamma \tag{3}$$

where Γ is the thermodynamic correction factor

$$\Gamma \equiv \frac{d\ln p}{d\ln\Theta} \tag{4}$$

The thermodynamic factor Γ can be determined from knowledge of the adsorption isotherm that relates the molecular loading Θ to the bulk gas pressure p.

Both Fick and M−S diffusivities are strongly dependent on the loading Θ, and this dependence is determined inter alia by molecule−molecule interactions, zeolite topology, and connectivity as evidenced by both MD simulations and experiments.[5−9] For guest−host systems, for which the isotherm exhibits inflection behavior, simulation studies have shown that this inflection is reflected in the loading dependence of both the Fick and the M−S diffusivities.[9−13] For diffusion of benzene in MFI, for example, the experiments of Shah et al.[14] show that the Fick diffusivity exhibits a sharp *maximum* at a loading $\Theta = 4$ molecules per unit cell; at this loading there is a sharp isotherm inflection. The maximum in the Fick D is attributable to the sharp maximum in the thermodynamic factor Γ at $\Theta = 4$.[10] The experimental investigation of Shah et al.[14] is the only one that we are aware of in which a sharp maximum in the Fick diffusivity has been reported.

In recent years Quasi-Elastic Neutron Scattering (QENS)[15] has proved to be a potent technique to probe the loading dependence of diffusivities of a variety of guest molecules in various zeolites.[5,6,9,16−20] In the present study, we use the QENS technique to investigate the loading dependence of both the Fick and self-diffusivities of nC6 and nC7 in MFI zeolite at 300 K. Our first major objective is to demonstrate that the Fick diffusivity exhibits a sharp maximum when the isotherm inflection is severe, as is the case for nC7.[13,21,22] Our second objective is to show that QENS can be used to determine the

* Corresponding author. Fax: + 31 20 5255604. E-mail: r.krishna@uva.nl.
[†] Institut de Recherches sur la Catalyse.
[‡] Institut Français du Pétrole.
[§] University of Amsterdam.

10.1021/jp055668k CCC: $33.50 © 2006 American Chemical Society
Published on Web 01/13/2006

inverse of the thermodynamic factor Γ from the coherent structure factor $S(Q)$. CBMC and MD simulations are also performed for comparison with the QENS results, with the final objective of determining to what extent simulations are able to match experiments.

2. QENS Experiments

The MFI zeolite (all silica version silicalite-1) sample was activated by heating it to 773 K under flowing oxygen. After cooling, the zeolite was pumped to 10^{-4} Pa, while heating it again to 773 K. Several samples were prepared by adsorbing known amounts of *n*-alkane onto the activated zeolite. For *n*-hexane, both hydrogenated and perdeuterated molecules were studied, the loadings correspond to the following numbers of molecules per unit cell: 2, 4, 6, and 8 C_6H_{14}, and 1, 2, 3, 4, 5, 6, 7, and 8 C_6D_{14}. For *n*-heptane, only the perdeuterated molecule was studied, the samples correspond to 0.9, 1.8, 2.7, 3.6, 4.5, 5.4, and 6.3 molecules per unit cell, on average. In view of the large amounts of MFI used for each sample, 4−8 g, the accuracy on the loadings is estimated to be 10%, in the worst case. The samples were transferred, inside a glovebox, into aluminum containers of annular geometry. The thickness of the zeolite powder was different between the hydrogenated and perdeuterated *n*-hexane samples, it was selected to give neutron transmissions ranging between 85 and 95%. All samples were equilibrated at 400 K during 4 h. Cells containing the dehydrated zeolite with the same amounts as for the loaded samples were also prepared. Their signal was subtracted from the spectra recorded with the cells containing the *n*-alkanes, for the same zeolite powder thickness, after normalization and corrections from neutron absorption.

The neutron experiments were performed on the backscattering spectrometer IN16 at the Institut Laue-Langevin, Grenoble. The containers were placed in a cryofurnace. The incident neutron energy was 2.08 meV (6.27 Å), using a Si(111) monochromator. Quasi-elastic measurements were performed by applying a Doppler shift to the incident neutrons through a movement of the monochromator. Spectra were recorded at different scattering angles, corresponding to wavevector transfer values, Q, ranging from 0.19 to 1.8 Å^{-1}. The resolution function could be fitted with a Gaussian function so that analytical convolution was employed. The full width at half-maximum of the energy resolution is of the order of 1 μeV, depending on the scattering angle. The energy transfer was analyzed in a window of ± 14 μeV.

When a sample contains different types of isotopes, the intensity measured by neutron scattering can be split into coherent and incoherent contributions

$$\frac{d^2\sigma}{d\Omega\, dE} = \frac{k_1}{k_0}\frac{1}{4\pi\hbar}[\sigma_{coh}S_{coh}(Q,\omega) + \sigma_{inc}S_{inc}(Q,\omega)] \quad (5)$$

where σ_{coh} and σ_{inc} are the coherent and incoherent scattering cross-sections, respectively. The neutron momentum transfer, $\hbar Q$, is defined by $\boldsymbol{Q} = \boldsymbol{k}_1 - \boldsymbol{k}_0$, where $\boldsymbol{k}_0$ and $\boldsymbol{k}_1$ are the incident and final wave vectors, respectively. Similarly, $\hbar\omega$ is the neutron energy transfer. $S(Q,\omega)$ is called the scattering function, or dynamical structure factor. The intensity of the coherent scattering is governed by the coherent structure factor, $S(Q)$, which is defined by the integral

$$S(Q) = \int_{-\infty}^{+\infty} S_{coh}(Q,\omega)\, d\omega \quad (6)$$

When the molecule contains hydrogen atoms, the scattering is essentially incoherent because of the large incoherent cross-section of this element (82 barns). One can then probe the dynamics of an individual proton or molecule. Coherent scattering involves interference effects between the waves scattered by different nuclei. In terms of correlation functions, it corresponds to the auto-correlation function of the particle density.

3. CBMC and MD Simulation Methodologies

CBMC and MD Simulations have been carried out for nC6 and nC7 alkanes in MFI (all silica silicalite-1) at 300 K; the crystallographic data are available elsewhere.[23,24] For both adsorption and diffusion simulations we use the united atom model. The zeolite framework is considered to be rigid. We consider the CH_x groups as single, chargeless interaction centers with their own effective potentials. The beads in the chain are connected by harmonic bonding potentials. A harmonic cosine bending potential models the bond bending between three neighboring beads, a Ryckaert−Bellemans potential controls the torsion angle. The beads in a chain separated by more than three bonds interact with each other through a Lennard−Jones potential. The Lennard−Jones potentials are shifted and cut at 12 Å. Pure component adsorption isotherms for alkanes were determined using CBMC simulations. The CBMC simulation details, along with the force fields have been given in detail in earlier publications.[21,22] The simulation box consists of $2 \times 2 \times 4$ unit cells and periodic boundary conditions were employed. It was verified that the size of the simulation box was large enough to yield reliable data on adsorption and diffusion. The inverse of the thermodynamic factor $1/\Gamma$ was determined from the CBMC simulations using the fluctuation formula derived by Reed and Ehrlich[25]

$$\frac{1}{\Gamma} = \frac{\langle N^2\rangle - \langle N\rangle^2}{\langle N\rangle} \quad (7)$$

where N represents the number of molecules in the simulation box and $\langle ... \rangle$ denotes ensemble averaging. This fluctuation formula has recently been used in Monte Carlo simulations for adsorption in zeolites.[26]

Diffusion in a system of N molecules is simulated using Newton's equations of motion until the system properties, on average, no longer change in time. The Verlet algorithm is used for time integration. The energy drift of the entire system is monitored to ensure that the time steps taken were not too large. A time step of 1 fs was used in all simulations. N molecules are inserted into the framework at random positions as long as no overlaps occur with the framework or other particles, and as long as the positions are accessible from the main cages and channels. During the initializing period we perform an NVT MC simulation to rapidly achieve an equilibrium molecular arrangement. After the initialization step, we assign velocities to the pseudo-atoms from the Maxwell−Boltzmann distribution at the desired average temperature. The total momentum of the system is set to zero. Next, we equilibrate the system further by performing an NVT MD simulation using the Nosé-Hoover thermostat. When the equilibration is completed, the production run starts. For every cycle, the statistics for determining the mean square displacements (MSDs) are updated. The MSDs are determined for time intervals ranging from 2 fs to 1 ns. To do this, an order-N algorithm, as detailed in Frenkel and Smit[27] is implemented. The details on how diffusivities are determined from the MSDs are also to be found in Frenkel and Smit[27] and elsewhere.[12,24] The Nosé-Hoover thermostat is used to main constant temperature conditions.

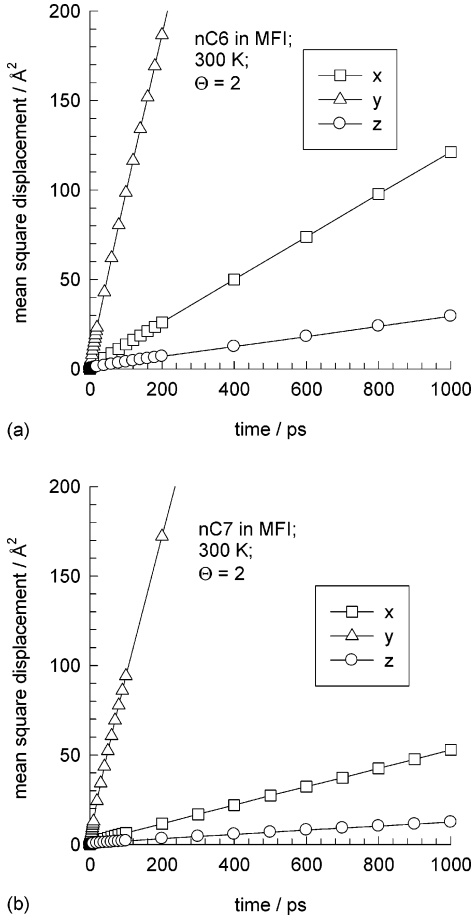

Figure 1. Mean square displacements (MSDs) for (a) nC6 and (b) nC7 in MFI at 300 K and loading $\Theta = 2$ molecules per unit cell. The open symbols represent the MSDs in each of the three coordinate directions.

The self-diffusivity, D_{self}, was computed by analyzing the MSDs of each component for each of the three coordinate

$$D_{self} = \frac{1}{2N}\lim_{\Delta t\to\infty}\frac{1}{\Delta t}\langle(\sum_{i=1}^{N}(\mathbf{r}_i(t+\Delta t) - \mathbf{r}_i(t))^2)\rangle \qquad (8)$$

directions, *x*, *y*, and *z*. In eq 8 this expression N represents the number of molecules, and $\mathbf{r}_i(t)$ is the position of molecule i at any time t. Typical MSDs, for each of the three coordinate directions, for nC6 and nC7 are shown in Figure 1a and b. We note that the diffusion is dominated by motion along the straight channels, in the *y*-direction. The M−S diffusivity Đ is determined from the formula for collective motion

$$Đ = \frac{1}{2}\lim_{\Delta t\to\infty}\frac{1}{N}\frac{1}{\Delta t}\langle(\sum_{i=1}^{N}(\mathbf{r}_i(t+\Delta t) - \mathbf{r}_i(t)))^2\rangle \qquad (9)$$

for each of the three coordinate directions, *x*, *y*, and *z*. The values of the M−S and self-diffusivities repeated in this paper represent averages over the three coordinate directions, e.g. $Đ = (Đ_x + Đ_y + Đ_z)/3$.

For any specified loading five independent MD simulations (each running for 72 h on PCs equipped with Intel Xeon processors running at 3.4 GHz on the Linux operating system) were carried out to obtain good estimates of diffusivities and standard deviations of the results.

4. Results and Discussion

The CBMC simulations for the adsorption isotherms are shown in Figure 2. Earlier publications have presented detailed comparisons of experimental results with CBMC simulations to demonstrate the accuracy of simulations;[21,22,28] these comparisons are, therefore, not repeated here. The isotherm for nC6 shows a slight inflection whereas that for nC7 shows a pronounced inflection. The reason for the inflection behavior of nC6 and nC7 has been attributed to "commensurate freezing", caused by the fact that the size (length) of these molecules is commensurate with that of the zigzag channels of MFI.[21,29] The isotherms conform reasonably well to the dual-site Langmuir (DSL) isotherm with fitted DSL model parameters as specified

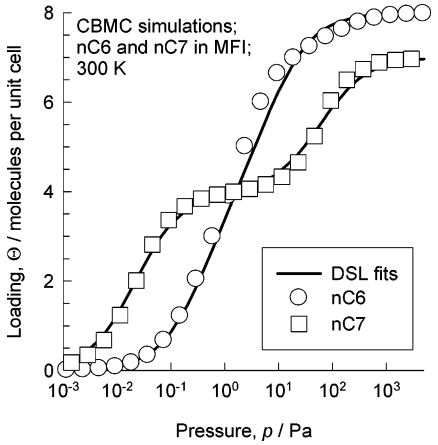

Figure 2. CBMC simulations (open symbols) of the sorption isotherms for nC6 and nC7 in MFI at 300 K. The continuous solid lines represent the dual-site Langmuir fits of the isotherms with the parameter values specified in Table 1.

TABLE 1: Dual-site Langmuir Parameters for *n*-alkanes in MFI at 300 K.[a]

	dual-site Langmuir parameters			
	b_A	$\Theta_{sat,A}$	b_B	$\Theta_{sat,B}$
nC6	2.5	4.0	0.15	4.0
nC7	45	4	0.017	3

[a] The Saturation Capacity Θ_{Sat} Has the Units of Molecules Per Unit Cell. The Langmuir Parameters b_A, b_B Have the Units of Pa^{-1}.

$$\Theta(p) \equiv \Theta_A + \Theta_B;\ \Theta_A = \frac{\Theta_{sat,A} b_A p}{1 + b_A p};\ \Theta_B = \frac{\Theta_{sat,B} b_B p}{1 + b_B p} \qquad (10)$$

in Table 1. In eq 10 b_A and b_B represent the DSL model parameters and the subscripts A and B refer to two sorption sites within the MFI structure, with different sorption capacities and sorption strengths. The $\Theta_{sat,A}$ and $\Theta_{sat,B}$ represent the saturation capacities of sites A and B, respectively. We can rewrite eq 10 as a quadratic expression in terms of the pressure:

$$(\Theta_{sat,A} + \Theta_{sat,B} - \Theta)b_A b_B p^2 + ((\Theta_{sat,A} - \Theta)b_A + (\Theta_{sat,B} - \Theta)b_B)p - \Theta = 0 \qquad (11)$$

The pressure for a given total loading Θ within the zeolite can be obtained from the physically feasible solution to eq 11

$$p = \frac{1}{2\alpha}(\sqrt{\beta^2 + 4\alpha\Theta} - \beta) \qquad (12)$$

where

$$\alpha = (\Theta_{sat,A} + \Theta_{sat,B} - \Theta)b_A b_B;\ \beta = (\Theta_{sat,A} - \Theta)b_A + (\Theta_{sat,B} - \Theta)b_B \qquad (13)$$

Using eq 4, we can obtain the inverse of the thermodynamic factor Γ in the convenient form

$$\frac{1}{\Gamma} = \frac{\Theta_A}{\Theta}\left(1 - \frac{\Theta_A}{\Theta_{A,sat}}\right) + \frac{\Theta_B}{\Theta}\left(1 - \frac{\Theta_B}{\Theta_{B,sat}}\right) \qquad (14)$$

Eqs 10, 12, 13, and 14 allow $1/\Gamma$ to be calculated explicitly as a function of the total loading Θ. The continuous solid lines in Figure 3a,b show the calculations of $1/\Gamma$ for nC6 and nC7 respectively using the fitted DSL parameters listed in Table 1. Also shown by open symbols in Figure 3a,b are the $1/\Gamma$ obtained from CBMC simulations using the fluctuation formula (7). It will be shown below how the thermodynamic factor can be derived from the neutron scattering measurements.

The scattered intensity measured for the samples containing C_6H_{14} is dominated by the incoherent scattering from the hydrogen atoms. The spectra obtained at the various loadings can be fitted with a single Lorentzian function, corresponding to self-diffusion, convoluted with the instrumental resolution function. Rotational motions occur on much shorter time scales[30] so that they only contribute to the scattering as a flat background in our limited energy window. All the spectra can be fitted simultaneously using the jump diffusion model described already.[18] For the deuterated *n*-alkanes, the situation is more complicated. The scattering cross-section of a carbon atom is totally coherent (5.554 barns), but the cross-section of a deuterium atom is both coherent and incoherent (5.597 and 2.04 barns, respectively). The coherent structure factor, $S(Q)$, which governs the intensity from coherent scattering, is also equal to the inverse of the thermodynamic factor, Γ, in the limit of zero wave vector transfer[6,31]

$$S(Q)_{Q\to 0} = \frac{d \ln \Theta}{d \ln p} = \frac{1}{\Gamma} \qquad (15)$$

The extrapolated value of $S(Q)$ and the thermodynamic factor can be related because they both correspond to a measure of the fluctuations of the number of molecules contained in a given volume.[25,32] The kinetic theory of gases relates particle fluctuations to the isothermal compressibility. Therefore, at small Q values, one expects a larger scattering power at small loadings (the sorbate phase is highly compressible like in a gas) than at saturation (a case similar to a liquid which is poorly compressible, and which is known to give small neutron intensities).

The filled symbols in Figure 3a,b represent the calculations of $1/\Gamma$ from the experimental intensities measured at small wave vector transfer using eq 15 for (a) C_6D_{14} and (b) C_7D_{16}. The $S(Q)$ values shown in Figure 3a,b are not exactly comparable to the inverses of the thermodynamic factors because one cannot measure scattered intensities at $Q = 0$. Further, the integration over energy transfers, as defined in eq 6, is only partial on a backscattering spectrometer, especially at high loadings where the signal becomes broader than the energy window. Nevertheless, the trends are similar in both sets of data, even if one takes account of experimental errors. For nC6, the inflection at $\Theta =$ 4 molecules per unit cell is more clearly revealed in Figure 3a than in the CBMC simulated isotherm in Figure 2 because of the derivative involved in the $1/\Gamma$ calculation. For nC7, the "step" obtained in the isotherm at $\Theta = 4$ leads to near-zero values for $S(Q)$ and for $1/\Gamma$, indicating a stable configuration of the molecules in the channels; see Figure 3b.

For C_6H_{14}, the total intensity integrated over the quasi-elastic domain increases continuously with the number of adsorbed molecules. In the case of coherent scattering, the effect of multiplying $S(Q)$, which is the intensity scattered by one molecule, with the number of scattering molecules results in a more complex intensity pattern. For C_2D_6 in MFI, whose adsorption isotherm can be described up to high loadings by a single-site Langmuir model, $1/\Gamma$ is linear, so that multiplying $S(Q)$ with the number of adsorbed molecules results for the total measured intensity in a single maximum around six molecules per unit cell.[9] For C_7D_{16}, one observes, for the first time, a double maximum for the total measured intensity, in keeping with the prediction obtained from the CBMC simulated isotherm; see Figure 4. As expected, the measured intensity shows a minimum for the intermediate loading $\Theta = 3.6$. Such a variation in intensity has never been reported before. It backs the general opinion that coherent neutron scattering is more complex than incoherent scattering.

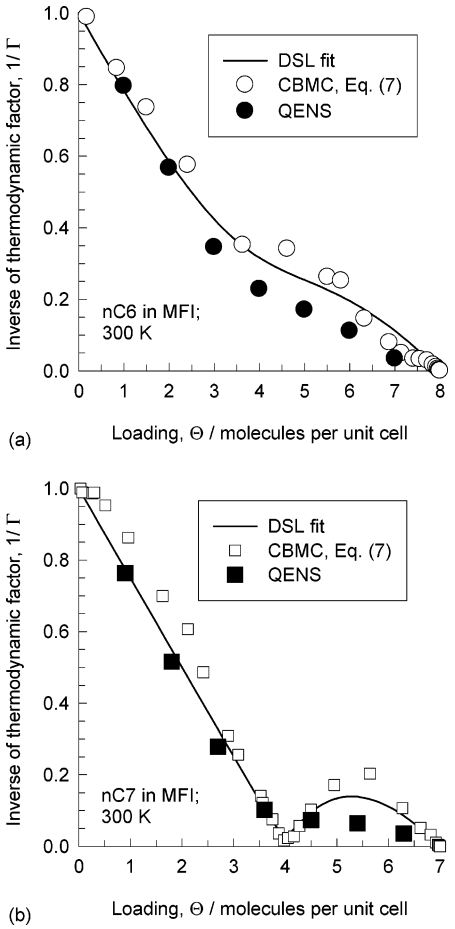

Figure 3. The continuous solid lines represent the inverse of the thermodynamic factor, $1/\Gamma$, as function of the molecular loading, using calculations following eq 14 for (a) C_6D_{14} and (b) C_7D_{16}. The open symbols are the values of $1/\Gamma$ determined from CBMC simulations using the Reed−Ehrlich fluctuation formula (7). The filled symbols in (a) and (b) are the intensities per unit scatterer, or $S(Q)$, measured at $Q = 0.19$ Å^{-1} from QENS data and calculated using eq 15.

The extraction of the diffusivity data from the QENS spectra needs special attention and requires further elaboration. When $S(Q)$ is large, the QENS spectra measured with deuterated molecules are dominated by coherent scattering. The data can be fitted with a single Lorentzian function, corresponding to transport diffusion. This is shown in Figure 5 in the case of C_7D_{16}, at loadings of (a) $\Theta = 0.9$, and (b) $\Theta = 1.8$. When $S(Q)$ is small, as is the case for higher loadings $\Theta = 3.6$, 4.5, 5.4, and 6.3, the spectra cannot be anymore fitted with only a single Lorentzian function; see Figure 6a. The contribution from incoherent scattering has then to be taken into account. This introduces a second component in the refinement, it corresponds

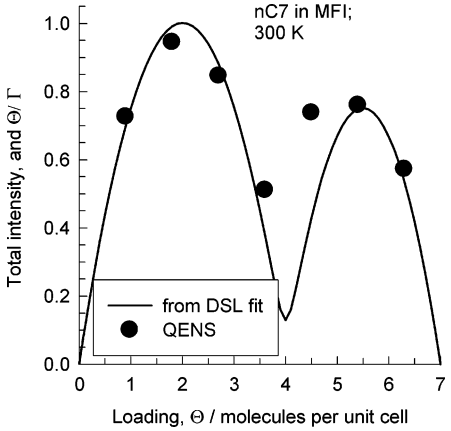

Figure 4. Experimental intensities integrated over the quasi-elastic peak at $Q = 0.19$ Å^{-1} for C_7D_{16} in MFI at 300 K (symbols) compared with Θ/Γ calculated from the DSL fit for nC7 using parameter values in Table 1.

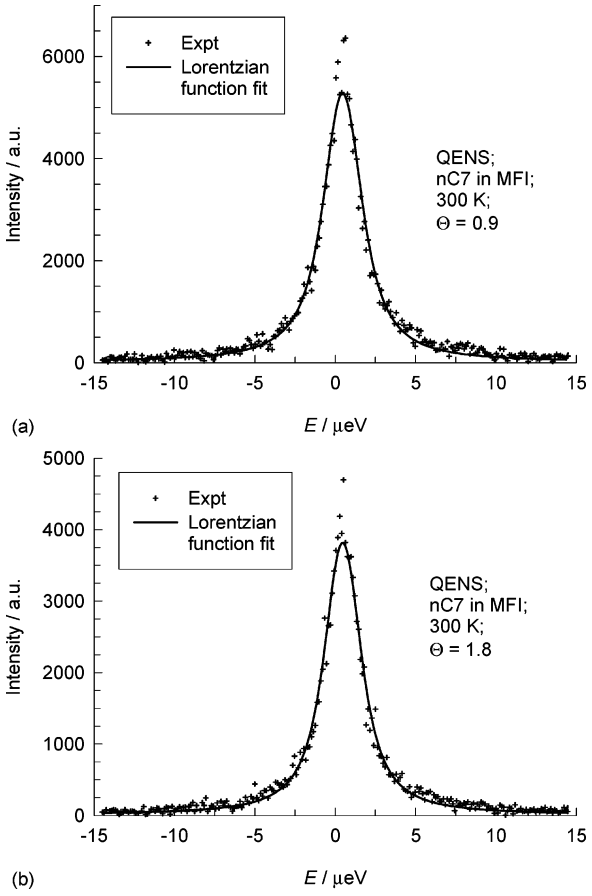

Figure 5. Comparison between experimental and fitted QENS spectra obtained at $Q = 0.19$ Å^{-1} for C_7D_{16} in MFI at 300 K at average loadings of (a) 0.9 and (b) 1.8 molecules per unit cell.

to the narrow Lorentzian function in Figure 6b. Because the spectra have to be fitted with two Lorentzian functions, the error bars on the Fick diffusivity values are larger. On the other hand, this allows to estimate the self-diffusivity, as was done with D_2 in NaX zeolite.[5]

The data on Fick, M−S, and self-diffusivities for nC6 and nC7 obtained from MD simulations and those extracted from QENS are compared in Figures 7 and 8. The MD simulated Fick diffusivity is obtained from $D = Đ\Gamma$ whereas the QENS M−S data is calculated from $Đ = D/\Gamma$. In both cases, the thermodynamic factor Γ is obtained from the DSL fit of simulated isotherms.

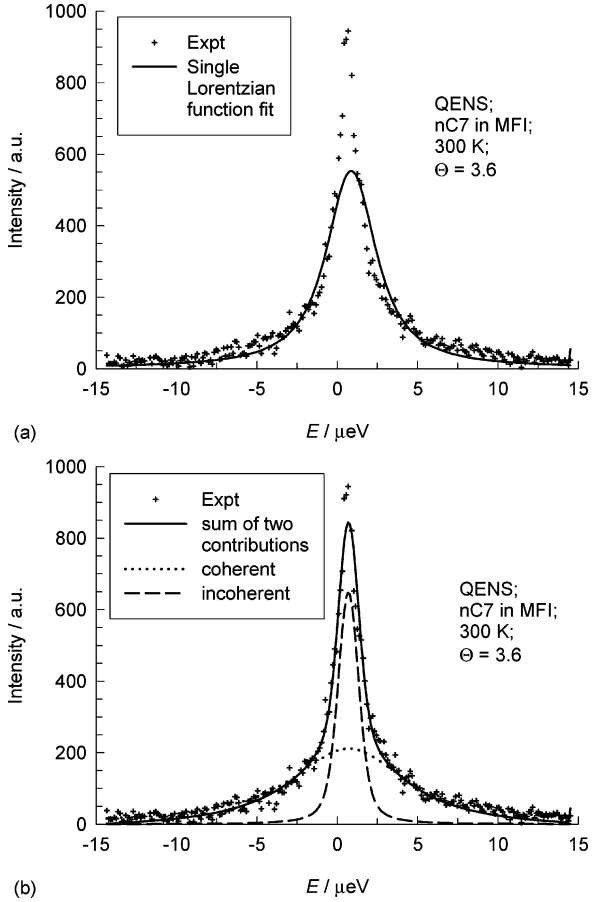

Figure 6. Comparison between experimental and fitted QENS spectra obtained at $Q = 0.19$ Å^{-1} for C_7D_{16} in MFI for an average loading of 3.6 molecules per unit cell. (a) The continuous solid line represents fit with only one Lorentzian function, convoluted with the instrumental resolution. (b) The continuous solid line represents sum of two Lorentzian functions, corresponding to coherent (dotted) and incoherent (dashed) contributions.

The slight inflection in the nC6 isotherm, evidenced by the inflection in $1/\Gamma$ (cf. Figure 3a) does not manifest by influencing the loading dependences of D, $Đ$, and D_{self}; see Figure 7a,b,c. The nC6 self-diffusivities were extracted from QENS data in two different ways: from the incoherent scattering of the hydrogenated molecules, and from the incoherent contribution observed at high loadings for the perdeuterated molecules. The two sets of values are shown with different symbols in Figure 7c. The MD simulated self-diffusivities for nC6 obtained in this work are in good agreement with those published recently by Leroy et al.[33] (the values plotted in Figure 7c represent their data for rigid MFI framework; the data for flexible framework are nearly the same); small differences between the two sets of MD simulations can perhaps be attributed to the use of different force fields.

For all three sets of nC6 diffusivities, the loading dependence found in the QENS experiments match those exhibited in the MD simulations. The MD simulated diffusivities are, however, about an order of magnitude higher than those obtained from QENS. Similar discrepancies between QENS experiments and MD simulations of self-diffusivities at near-zero loadings have been observed in the published literature for linear alkanes in MFI with C numbers higher than four.[18,34,35] A recent comparison between experimental results and simulations points out the influence of internal diffusion barriers in MFI-type zeolites.[36] Vlugt et al.[37] have demonstrated that simulated values of

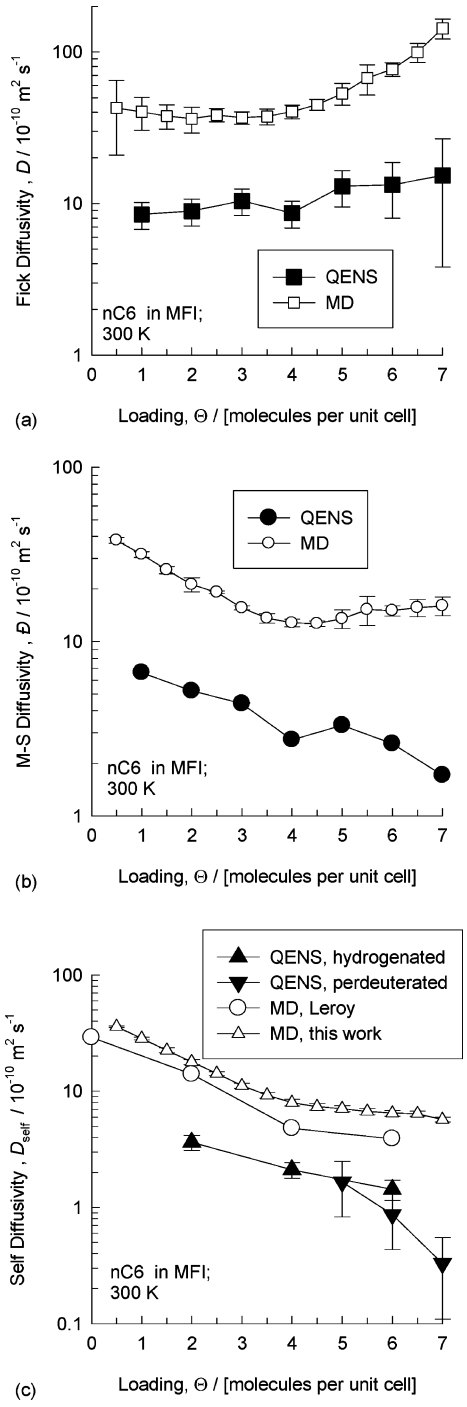

Figure 7. Comparison of the QENS and MD simulated (a) Fick, (b) M−S and (c) self-diffusivities for *n*-hexane in MFI at 300 K.

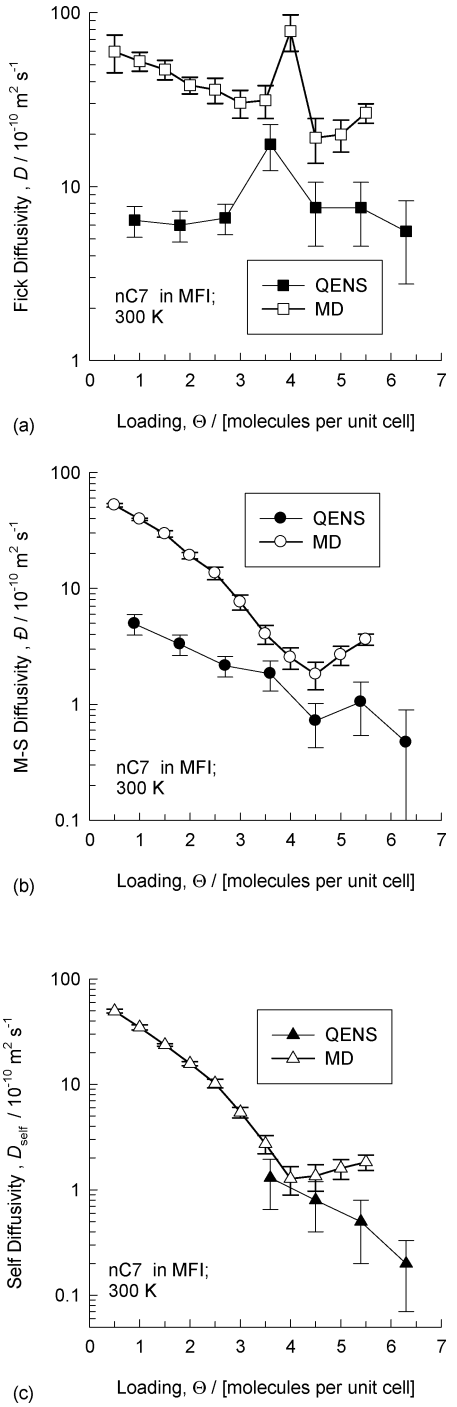

Figure 8. Comparison of the QENS and MD simulated (a) Fick, (b) M−S, and (c) self-diffusivities for *n*-heptane in MFI at 300 K.

diffusivity in MFI are extremely sensitive to small variations in the value of the Lennard−Jones parameter σ.

As a consequence of the fact that the isotherm for nC7 shows a severe inflection at $\Theta = 4$ (cf Figure 2 and Figure 3b), the Fick diffusivity D exhibits a sharp maximum in the region of $\Theta = 4$, evidenced equally in the MD and QENS data; see Figure 8a. This maximum is entirely analogous to that observed in the experiments of Shah et al.,[14] for Fick diffusivity of benzene in MFI $\Theta = 4$. The nC7 isotherm inflection also causes an inflection in the loading dependence of the M−S diffusivity Đ (cf. Figure 8b), observed both in MD and QENS data, in conformity with the earlier developed model.[11] The MD simulated D_{self} for nC7 also exhibits inflection behavior at $\Theta = 4$ (cf. Figure 8c) but a confirmation of this inflection is not evident in the QENS data due to the fact that self-diffusivities could only obtained from QENS at high loadings. As for nC6, the magnitudes of the MD simulated diffusivities for nC7 are about five times higher than those obtained from QENS.

5. Conclusions

In this study we have probed the adsorption and diffusion characteristics of nC6 and nC7 in MFI zeolite using both QENS and molecular simulations (CBMC and MD). The following major conclusions emerge from this study.

(a) The inverse of the thermodynamic factor, Γ, can be obtained from the coherent structure factor, $S(Q)$, in the limit of zero wave vector transfer. For nC6 and nC7 the value of $1/\Gamma$

thus obtained from QENS is in reasonably good agreement with that obtained from CBMC simulations using the Reed−Ehrlich fluctuation formula (7), and also that calculated using eq 14 with DSL fit parameters listed in Table 1.

(b) The loading dependence of the Fick, M−S and self-diffusivities of both nC6 and nC7 obtained from QENS data show good qualitative match with those from MD simulations. The magnitudes of the diffusivities from MD simulations are about a factor of five higher than the QENS values. Similar discrepancies in the self-diffusivities at near-zero loadings were observed in the published literature.[18,34,35] Further work will be required to reconcile these differences.

(c) For nC6, the isotherm inflection is not strong enough to have a significant influence on the loading dependence of diffusivities.

(d) *n*-Heptane shows a strong isotherm inflection at a loading of $\Theta = 4$. Consequently, at this loading both QENS and MD simulation data on the M−S diffusivity shows inflection in its loading dependence. Also, Fick diffusivity shows a sharp maximum at $\Theta = 4$. The practical implications of such loading dependences of M−S and Fick diffusivities of alkanes in MFI have been explored in the published literature.[2,10]

Acknowledgment. The neutron experiments were performed at the Institut Laue-Langevin, Grenoble, France, using the IN16 spectrometer. We thank Dr. B. Frick for his help during the measurements. R.K. acknowledges the grant of a TOP subsidy from the Netherlands Foundation for Fundamental Research (NWO-CW) for intensification of reactors and NWO/NCF for provision of high performance computing resources. R.K. also acknowledges D. Dubbeldam, S. Calero, T.J.H. Vlugt, E. Beerdsen, and B. Smit for providing the CBMC and MD simulation codes.

References and Notes

(1) Kärger, J.; Ruthven, D. M. *Diffusion in zeolites and other microporous solids*; John Wiley: New York, 1992.

(2) Krishna, R.; Baur, R. *Sep. Purif. Technol.* **2003**, *33*, 213−254.

(3) Keil, F. J.; Krishna, R.; Coppens, M. O. *Rev. Chem. Eng.* **2000**, *16*, 71−197.

(4) Skoulidas, A. I.; Sholl, D. S.; Krishna, R. *Langmuir* **2003**, *19*, 7977−7988.

(5) Jobic, H.; Kärger, J.; Bée, M. *Phys. Rev. Lett.* **1999**, *82*, 4260−4263.

(6) Papadopoulos, G. K.; Jobic, H.; Theodorou, D. N. *J. Phys. Chem. B* **2004**, *108*, 12748−12756.

(7) Skoulidas, A. I.; Sholl, D. S. *J. Phys. Chem. A* **2003**, *107*, 10132−10141.

(8) Krishna, R.; Paschek, D.; Baur, R. *Microporous Mesoporous Mater.* **2004**, *76*, 233−246.

(9) Chong, S. S.; Jobic, H.; Plazanet, M.; Sholl, D. S. *Chem. Phys. Lett.* **2005**, *408*, 157−161.

(10) Krishna, R.; Vlugt, T. J. H.; Smit, B. *Chem. Eng. Sci.* **1999**, *54*, 1751−1757.

(11) Krishna, R.; van Baten, J. M.; Dubbeldam, D. *J. Phys. Chem. B* **2004**, *108*, 14820−14822.

(12) Krishna, R.; van Baten, J. M. *J. Phys. Chem. B* **2005**, *109*, 6386-6396.

(13) Krishna, R.; Van Baten, J. M. *Chem. Phys. Lett.* **2005**, *407*, 159−165.

(14) Shah, D. B.; Guo, C. J.; Hayhurst, D. T. *J. Chem. Soc., Faraday Trans.* **1995**, *91*, 1143−1146.

(15) Bée, M. *Quasielastic Neutron Scattering*; Hilger: Bristol, 1988.

(16) Jobic, H.; Hahn, K.; Kärger, J.; Bee, M.; Tuel, A.; Noack, M.; Girnus, I.; Kearley, G. J. *J. Phys. Chem. B* **1997**, *101*, 5834−5841.

(17) Jobic, H.; Ernst, H.; Heink, W.; Kärger, J.; Tuel, A.; Bee, M. *Microporous Mesoporous Mater.* **1998**, *26*, 67−75.

(18) Jobic, H. *J. Mol. Catal. A: Chem.* **2000**, *158*, 135−142.

(19) Jobic, H.; Skoulidas, A. I.; Sholl, D. S. *J. Phys. Chem. B* **2004**, *108*, 10613−10616.

(20) Jobic, H.; Methivier, A.; Ehlers, G.; Farago, B.; Haeussler, W. *Angew. Chem., Int. Ed.* **2004**, *43*, 364−366.

(21) Vlugt, T. J. H.; Krishna, R.; Smit, B. *J. Phys. Chem. B* **1999**, *103*, 1102−1118.

(22) Dubbeldam, D.; Calero, S.; Vlugt, T. J. H.; Krishna, R.; Maesen, T. L. M.; Smit, B. *J. Phys. Chem. B* **2004**, *108*, 12301−12313.

(23) Baerlocher, C.; McCusker, L. B. *Database of Zeolite Structures.* http://www.iza-structure.org/databases/; International Zeolite Association, 2000.

(24) van Baten, J. M.; Krishna, R. *MD Simulations of Diffusion in Zeolites.* http://ct-cr4.chem.uva.nl/md/; University of Amsterdam, 2004.

(25) Reed, D. A.; Ehrlich, G. *Surf. Sci.* **1981**, *102*, 588−609.

(26) Chen, H.; Sholl, D. S. *Langmuir* **2005**, *In press*.

(27) Frenkel, D.; Smit, B. *Understanding molecular simulations: from algorithms to applications*, 2nd ed.; Academic Press: San Diego, 2002.

(28) Schenk, M.; Vidal, S. L.; Vlugt, T. J. H.; Smit, B.; Krishna, R. *Langmuir* **2001**, *17*, 1558−1570.

(29) Smit, B.; Maesen, T. L. M. *Nature* **1995**, *374*, 42−44.

(30) Jobic, H.; Bée, M.; Caro, J. *9th International Zeolite Conference, 1992, Montreal*; von Ballmoos, R., Higgins, J. B., Treacy, M. M. J., Eds; Butterworth-Heinemann: 1993; Vol. II, p 121.

(31) Hempelmann, R.; Richter, D.; Faux, D. A.; Ross, D. K. *Z. Phys. Chem. Neue Folge* **1988**, *159*, 175.

(32) Guisnet, A. *Théorie et technique de la radiocristallographie*; Dunod: Paris, 1964.

(33) Leroy, F.; Rousseau, B.; Fuchs, A. H. *Phys. Chem. Chem. Phys.* **2004**, *6*, 775−783.

(34) Maginn, E. J.; Bell, A. T.; Theodorou, D. N. *J. Phys. Chem.* **1996**, *100*, 7155−7173.

(35) Leroy, F.; Jobic, H. *Chem. Phys. Lett.* **2005**, *406*, 375−380.

(36) Jobic, H.; Schmidt, W.; Krause, C. B.; Kärger, J. *Microporous Mesoporous Mater.* In press.

(37) Vlugt, T. J. H.; Dellago, C.; Smit, B. *J. Chem. Phys.* **2000**, *113*, 8791−8799.